Mechanisms and Kinetics of Mechanical Alloying in Binary Powder Fe-M (M = B, C, Mg, Al, Si, Ge, Sn) Mixtures

E.P. Yelsukov, G.A. Dorofeev

Physical-Technical Institute UrB RAS, 426001 Izhevsk, Russia.

E-mail: yelsukov@fnms.fti.udm.ru

Common and distinctive features of mechanical alloying of Fe with sp-elements have been established using a complex of experimental methods.

The common regularities are following: the formation of a nanostructural state in α-Fe particles, sp-element penetration along the α-Fe grain boundaries, its segregation and the first Fe-M phase formation in the interfaces (boundary and close-to-boundary distorted zones) at the initial stage; the realization of any type of solid state reactions (SSR) only on reaching the nanocrystalline state.

The differences in the type of SSR and their kinetics are conditioned by the ratio of the covalent radii ($A_M=R_M/R_{Fe}$), external shell electron configuration of sp-atom and sp-element concentration (x_M) in the initial mixture.

In alloying α-Fe with sp-elements (Al, Si, Ge, Sn) having approximately equal and substantially larger atomic size (A_M=1.01; 0.95; 1.04; 1.21, respectively) the most stable intermetallic compounds are formed in interfaces at the first stage. At the final stage supersaturated solid solution (SSS) is formed in the grain bulk if $x_M \leq 32$at.% Si (Ge, Sn) and ≤50at.% Al. In the Fe-Al (Si, Ge) systems the sp-element concentration in SSS becomes maximum simultaneously with the SSS formation, while in the Fe-Sn system SSS is saturated with Sn gradually.

In contrast to the Fe-Al (Si, Ge, Sn) systems in α-Fe alloying with the C and B atoms of a small radius (A_M=0.66 and 0.70, respectively) an amorphous-like phase (Am(Fe-M)) is formed in interfaces at the initial stage. The Am(Fe-B) formation is characterized by a substantially slower kinetics in comparison with that of the Am(Fe-C) one. If x_M>15at.% C(B) the second stage – the carbide and boride formation – takes place after amorphization.

The work had been supported by the Russian Fund for Basic Research (projects 97-03-33483 and 00-03-32555).

MECHANICAL GRINDING AND ALLOYING

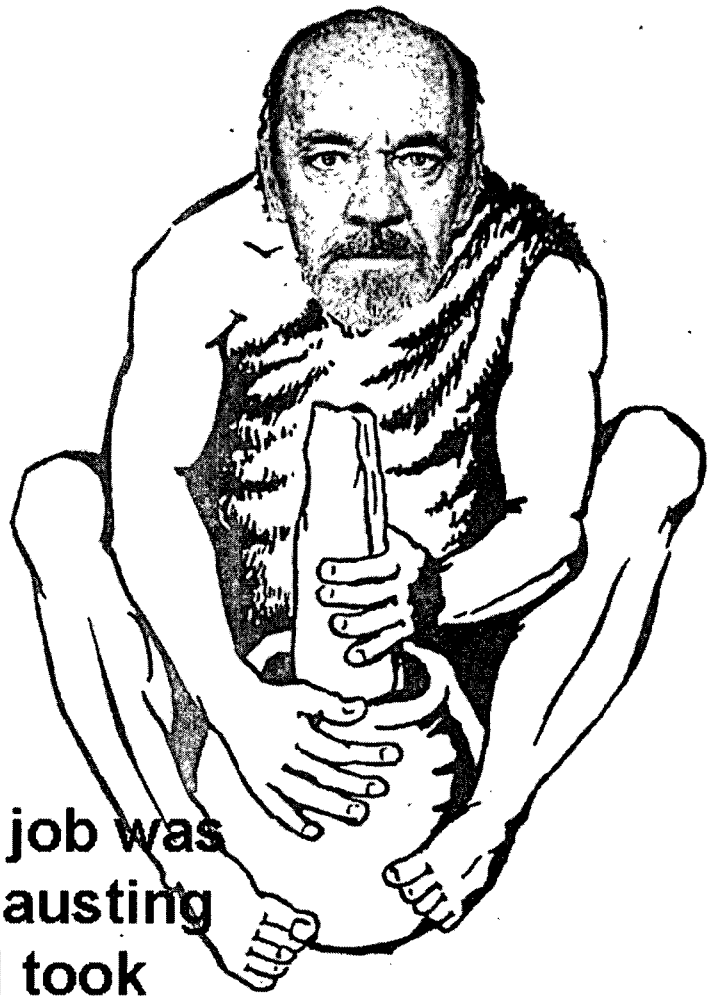

His job was exhausting and took much time ...

Mechanisms and Kinetics of Mechanical Alloying in Binary Powder Fe-M (M = B, C, Mg, Al, Si, Ge, Sn) Mixtures

E.P.Yelsukov, G.A.Dorofeev

Physical-Technical Institute UrB RAS, 426001, Izhevsk, Russia

Dr. G.N.Konygin Dr. A.L.Ulyanov Dr. V.A.Zagainov Dr. I.V.Povstugar	Physical-Technical Institute UrB RAS, Izhevsk, Russia
Prof. A.E.Yermakov Dr. V.A.Barinov	Institute of Metal Physics UrB RAS, Ekaterinburg, Russia
Prof. V.V.Boldyrev Prof. N.Z.Lyakhov Dr. T.F.Grigoryeva	Institute of Solid State Chemistry SB RAS, Novosibirsk, Russia
Prof. P.Yu.Butyagin Prof. A.N.Streletskii	Semenov Institute of Chemical Physics RAS, Moscow, Russia

Introduction

The questions:

1. What do we imply by the term "deformation atomic mixing"?

2. What are the major factors determining the kinetics of solid state reactions?

3. What are driving forces responsible for the supersaturated effects?

Appropriate model objects to answer these questions are binary powder mixtures of the Fe with sp-elements (M)

Why?

Individual properties of

	atoms			elements			
	Atomic weight	External electron shell	Covalent radius, Å	Lattice	Density, $g \cdot sm^{-3}$	Mechanical properties	T_{melt}, K
Fe	55.8	$3d^6 4s^2$	1.17	BCC	7.86	ductile	1808
B	10.8	$2s^2 p^1$	0.88	Tetrag.	2.34	brittle	2303
C	12.0	$2s^2 p^2$	0.77	HCP (graphite)	2.26	brittle	>4000
Mg	24.3	$3s^2 p^0$	1.30	HCP	1.74	ductile	923
Al	27.0	$3s^2 p^1$	1.18	FCC	2.70	ductile	933
Si	28.1	$3s^2 p^2$	1.11	Diamond	2.33	brittle	1683
Ge	72.6	$4s^2 p^2$	1.22	Diamond	5.32	brittle	1210
Sn	118.7	$5s^2 p^2$	1.41	Tetrag.	7.3	ductile	505
Pb	207.2	$6s^2 p^2$	1.47	FCC	11.4	ductile	600

Equilibrium phase diagrams

1. Extended concentration range of α-Fe(M) solid solution (SS), intermetallic compounds:

Fe-Al, Fe-Si and Fe-Ge.

2. Limited concentration range of α-Fe(M) SS, intermetallic compounds:

Fe-Sn.

3. Absence of the M solubility in the α-Fe, carbides and borides:

Fe-C and Fe-B.

4. Immiscible systems:

Fe-Mg and Fe-Pb.

5. Absence of the Fe solubility in the M materials.

Mechanical alloying (MA) in the Fe-M systems has been attracting much attention for the last 15 years.

However, detailed comparison of mechanisms and kinetics of MA on the basis of the earlier published data is not possible as:

1. MA was carried out under different conditions: the material of grinding tools, power intensity of mills and milling atmosphere;

2. There are considerable differences in the results published for some Fe-M systems.

The aim of this paper was to classify the results on the mechanisms and kinetics of MA in the Fe-M systems obtained in our laboratory under equal conditions of mechanical treatment taking into account the other authors' results as well.

Experimental

Initial powders with the particle size ≤300mm

The studied samples

- Fe(100-x)C(X); x=5, 10, 15, 17, 20, 25, 32 at.%
- Fe(100-x)B(x); x=15, 32 at.%
- Fe(100-x)Si(x); x=25, 32 at.%
- Fe(100-x)Ge(x); x=32, 50 at.%
- Fe(100-x)Sn(x); x=10, 25, 32 at.%
- Fe(68)Al(32)
- Fe(100-x)Mg(x); x=5, 7, 10, 15, 32 at.%
- Fe(95)Pb(5)

A planetary ball mill Fritsch P-7

- vials and balls made of hardened steel containing 1 wt.%C and 1.5wt.%Cr
- power intensity – 2Wt/g
- Loading – 10g
- atmosphere – Ar
- heating – ≤60°C

Experimental techniques

- post-milling mass increase measurements
- X-ray diffraction
- Mössbauer spectroscopy
- magnetic measurements
- Auger spectroscopy
- transmission electron microscopy
- Secondary ion mass spectrometry (SIMS): measuring chemical content in surface layer of particles
- Gross chemical analysis (CA) using a Spectra flame-Modula D atomic emission spectrometer

Thermodynamic calculations

- Miedema's model with taking into account the interfacial energy and grain boundary segregation of sp-elements

Mechanical grinding α-Fe

Initial state

Specific saturation magnetization	$\sigma = 217 A \cdot m^2 / kg$
Coercivity	$H_c = 10 Oe$
Particle size	$D \leq 300\ \mu m$
Grain size	$< L > \geq 100\ nm$
Carbon content	$\leq 0.02\ wt\%$

I. Milling in inert atmosphere (Ar)

Auger spectroscopy

a) Secondary electron microscopy mode image of particles;

b) Auger spectra of the surface (1) and after etching the surface layer 30 nm thick (2).

Milling for 34 hours.

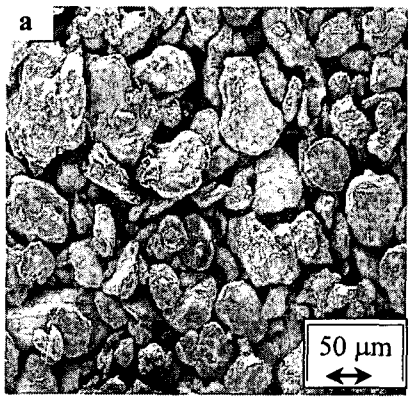

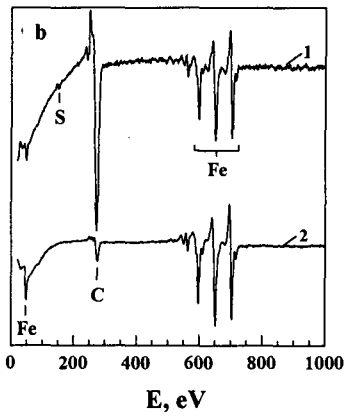

- The surface layers of the Fe powder particles are contaminated with carbon prior to and after milling.
- The less the size of the particles D before milling is, the higher the C content in the bulk of the particle after milling will be.

Mechanical grinding α-Fe

X-ray diffraction

(110) and (220) peaks of bcc structure

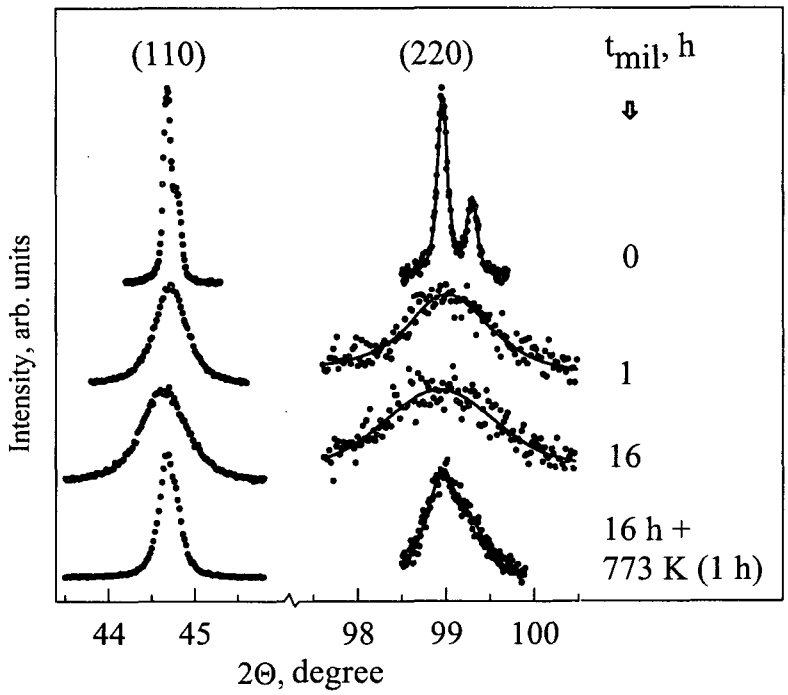

- <L> ≥ 100 nm (t_{mil} = 0); <L> = 9 nm (t_{mil} = 16 h);
- The bcc lattice parameter of the nanocrystalline Fe (t_{mil} = 16 h) a = 0.2869 nm;
- With the width of the interfaces d = 1 nm and <L> = 9 nm the volume fraction of the interfaces is ≡ 30 %;
- The lattice parameter of the interfaces is 1 % more than that of the grain bulks (0.2866 nm).

HREM: Al-3 % Mg

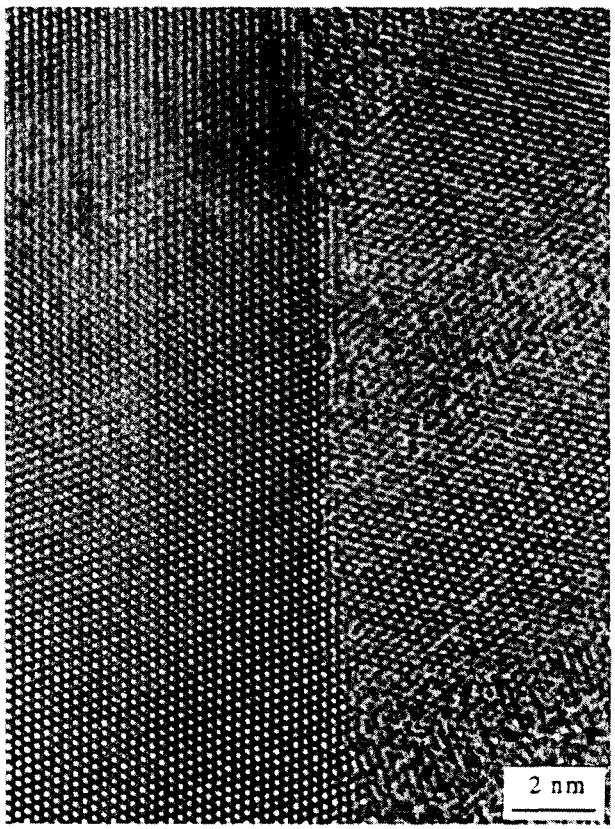

Grain boundary lattice image in as-strained condition

[*Horita Z., Smith D.J., Furakawa M., Nemoto M., Valiev R.Z., Langdon T.G. Materials Characterization, 1996, V. 37, p. 285*]

Mechanical grinding α-Fe

^{57}Fe Mössbauer spectroscopy

(a) - complete Mössbauer spectra
(b) - the 1st and 6th lines of the MS

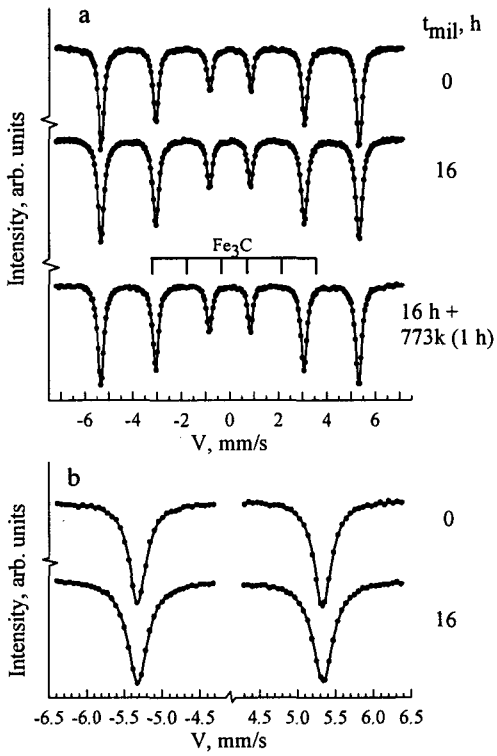

- Any second components is not available in the MS of the milled powders;
- Fe_3C carbide is not found after annealing of the milled samples;
- The width of the MS lines of the milled samples is by 20 % more than that of the initial Fe powder.

Mechanical grinding α-Fe

Structural and Mössbauer parameters of the Fe samples milled in Ar

Sample	*a*, nm	<L>, nm	$<\varepsilon^2>^{1/2}$, %	$\Gamma_{1,6}$, mm/s	δ, mm/s	Δ, mm/s	H, кЭ
Initial	0.2866_1	100_{10}	0.03_3	0.27_1	0.01_1	0.00_1	$331,0_5$
t_{mil}=1 h	0.2867_1	13_2	0.15_3	0.30_1	0.00_1	0.00_1	$331,1_5$
t_{mil}=16 h	0.2869_1	9_2	0.22_3	0.32_1	0.01_1	0.00_1	331.1_5
t_{mil}=16 h+ annealing 773K (1h)	0.2866_1	25_4	0.10_3	0.30_1	0.01_1	0.00_1	330.8_5

Summary (milling in Ar)

- Transition of α-Fe into a nanocrystalline state results in a small increase of the bcc lattice parameter, microstrain growth, increase of the MS lines width by 20 % and considerable changes in coercivity;
- All other parameters remain unchanged. There is no new component in MS;
- The increase of Γ can be accounted for by the appearance of a different in value and sign anysotropic contribution to HFMF for the Fe atoms in the close-to-boundary distorted zone

$$H = H_{is} + H_{anis}$$

$$H_{anis} = \frac{1}{2} h(3\cos^2\Theta - 1)$$

In the non-distorted bcc structure $\Theta = 54^0 30'$ and $H_{anis} = 0$. In distorted zone $\Theta \neq 54^0 30'$ and $H_{anis} \neq 0$.

Mechanical alloying Fe-C and Fe-B systems

Mechanical alloying Fe-C system

x, at.% C	Solid state reactions	Publications
8.7	Interstitial solid solution	Nadutov et al., Mater. Sci. Forum 343 - 346 (2000) 721
19.5	Interstitial solid solution	Shabashov et al. Matter. Sci. Engen. A307(2001) 91
≤15 20-25 50	Hexagonal Carbides (HC) HC+Fe_3C Fe_7C_3	Hyperfine Interact. 66(1991)309; Le Caër et al., Colloq. De Phys. 51 (1990) C4-151; J. Mater. Sci. 25 (1990) 4726
30	Fe_3C	Bokhonov et al. J.Alloys and Comp. 333(2002) 308
25, 28.6	$Fe_3C \rightarrow Fe_7C_3$	Tokumitzu, Umemoto, Mater. Sci. Forum 360-362 (2001) 183
17-25 29-50	Am(Fe-C)$\rightarrow Fe_3C$ Am(Fe-C)$\rightarrow Fe_7C_3$	Tanaka et al. J.Less-Comm. Met. 171(1991) 237
20 50	Am (Fe_3C)$\rightarrow Fe_3C$ $Fe_3C \rightarrow Fe_7C_3$	Wang et al., Mater. Sci. Forum 179 – 181 (1995) 201
25	Am (Fe_3C)$\rightarrow Fe_3C \rightarrow Fe_7C_3$	Campbell et al., Mater. Sci. Engen. A226 – 228 (1997) 75
32	Am (Fe-C)$\rightarrow Fe_3C \rightarrow Fe_7C_3$	Dorofeev et al., Phys. Chem. of Mater. Treatment (Russia) 5 (2001) 71
<17 17-25	Am(Fe-C) Am(Fe-C)$\rightarrow (Fe_3C)_D$	Elsukov et al. Phys. Met. Metallogr. 93(3) (2002) 278; 94(4) (2002) 356
25	Am(Fe-C)	Nasu et al., J.Non-Cryst. Sol. 122 (1990) 216; Mater. Sci. Engen. A134 (1991) 1385
20-25	Am(Fe-C)	Ogasawara et al., Mater. Sci. Engen. A134 (1991) 1338

Journal of the Less-Common Metals, 171 (1991) 237-247

Mechanical alloying of the high carbon Fe-C system

T. Tanaka
Department of Engineering, Osaka Sangyo University, Daito, Osaka 574 (Japan)

S. Nasu
Department of Metal Physics, Faculty of Engineering Science, Osaka University. Toyonaka, Osaka 560 (Japan)

K. N. Ishihara and P. H. Shingu
Department of Metal Science and Technology, Kyoto University. Yoshida Sakyo-ku, Kyoto 606 (Japan)

Fig. 2. Scanning electron micrographs of the cross-sectional structure of $Fe_{75}C_{25}$ powders ball milled for (a) 20 h

Mechanical Alloying Fe(85)C(15)

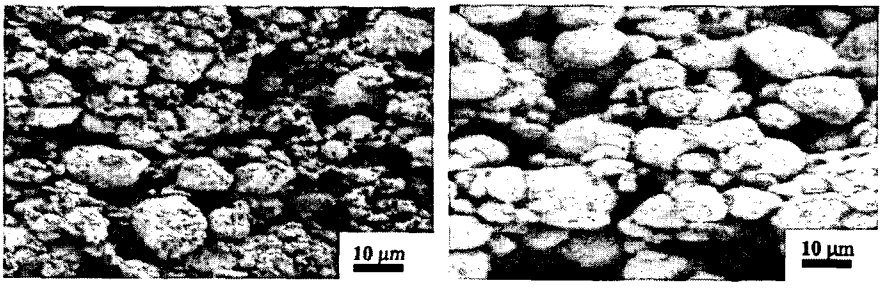

t_{mil} = 1 hour

t_{mil} = 16 hours

Secondary electron microscopy mode image of particles

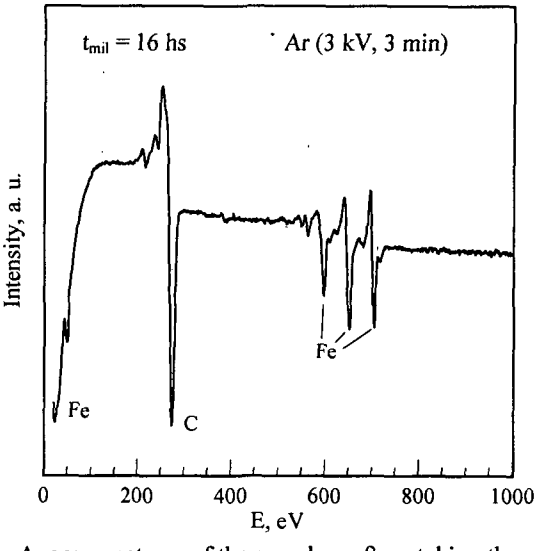

Auger-spectrum of the powders after etching the surface layer of 10 nm thick

Mechanical Alloying Fe(85)C(15)

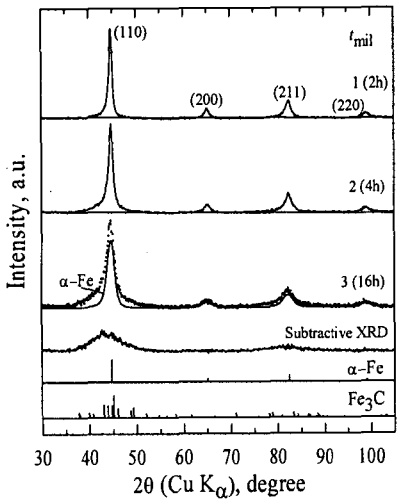

X-ray diffraction patterns

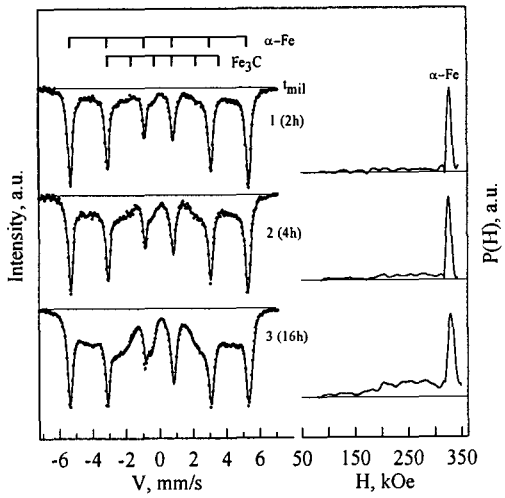

Mössbauer spectra and P(H) functions

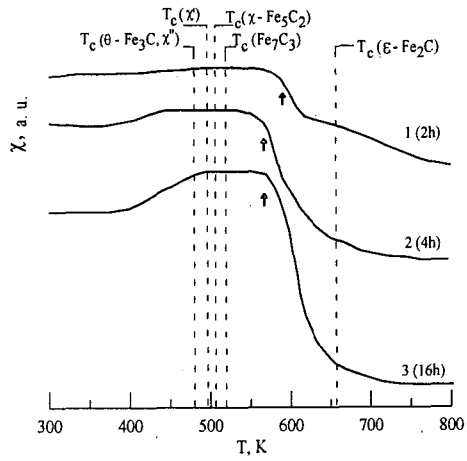

A.c. magnetic susceptibility

α-Fe + C
↓
nanocomposite
α-Fe + Am (Fe-C)
phase

Mechanical Alloying Fe(85)C(15) (t_{mil} = 16 hours)

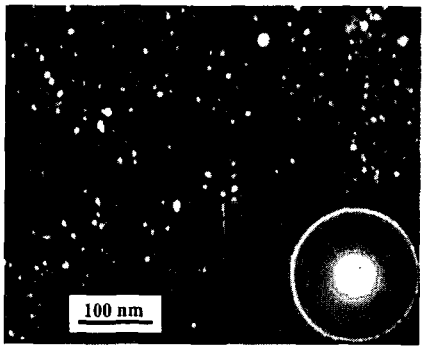

Dark-field electron micrograph and selected area diffraxction pattern

Isochronous (1 h) annealing (T_{ann} = 500 °C)

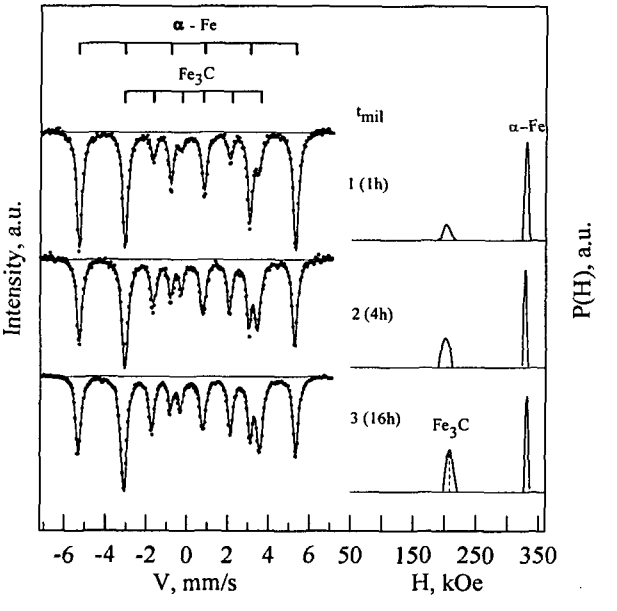

Mössbauer spectra and P(H) functions

Quantitive analysis of the MA process in the Fe(85)C(15) mixture

S_{Am} - Fe atomic fraction, $\overline{H}\,Am$ - average HFMF and x_{Am} - C concentration of amorphous Fe-C phase;

S_{Fe_3C} - Fe atomic fraction of Fe_3C carbide after MA followed by annealing at T_{ann} = 500 °C (1h).

t_{mil}, hours	S_{Am}, %	$\overline{H}\,Am$, kOe	x_{Am}, at.%	S_{Fe_3C}, %
1	14_3	220_5	27	28_3
2	31_3	225_5	26	46_3
4	41_3	236_5	24	52_3
8	52_3	238_5	24	55_3
16	54_3	238_5	24	54_3

x_b^{MA} - amount of carbon bound in the amorphous phase after MA;

x_b^{Ann} - amount of carbon bound in the cementite after MA followed by annealing at T_{ann} = 500 °C (1h);

$x_{ub} = x_b^{Ann} - x_b^{MA}$ - amount of carbon unbound in the α-Fe particles after MA;

<L> - grain size of α-Fe;

f_{Am} - atomic fraction of the amorphous phase;

f_{if} - volume fraction of interfaces.

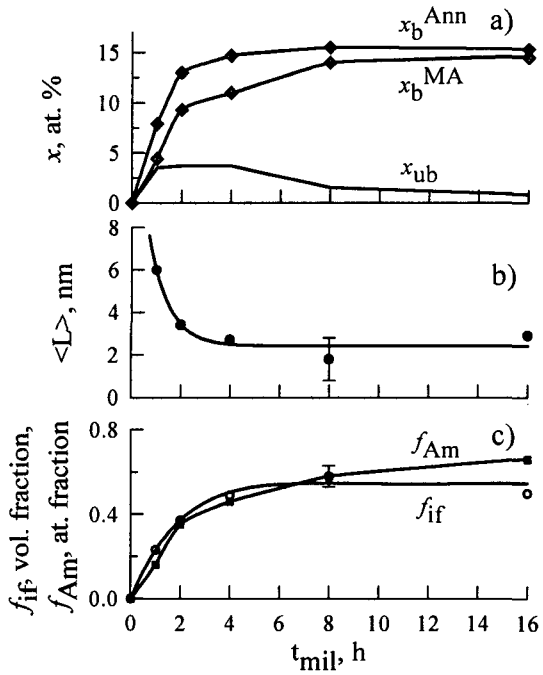

Mechanical alloying Fe (75)C(25)
t_{mil} = 16 hours (milling in Ar)

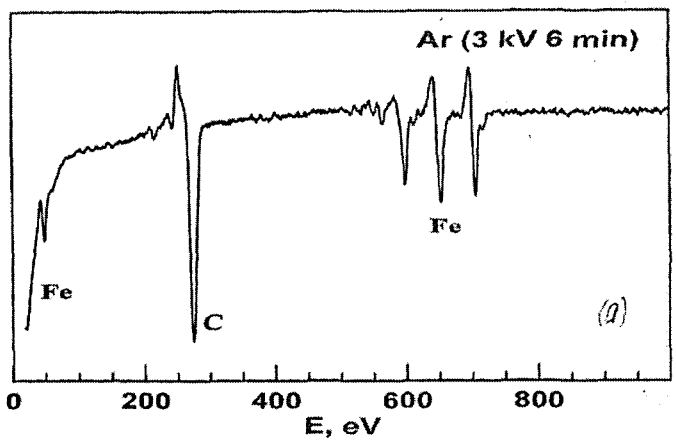

Auger - spectrum of the powder after etching
the surface layer of 20 nm thick

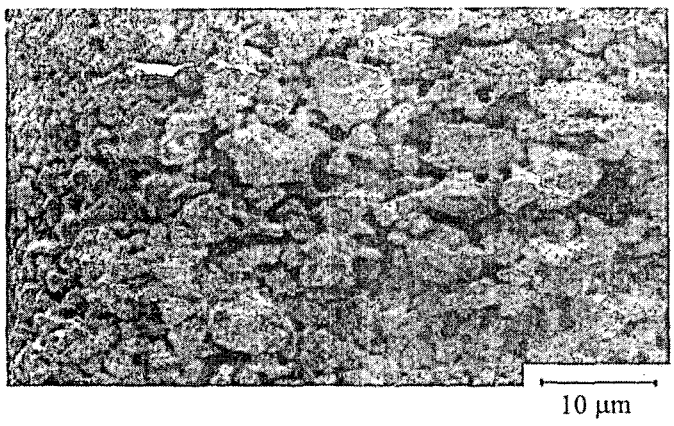

Secondary electron microscopy mode image of particles

Mechanical alloying in Fe(75)C(25)

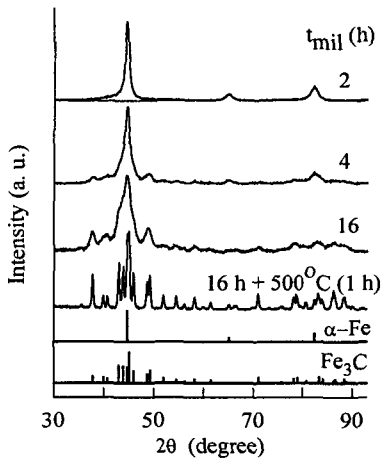

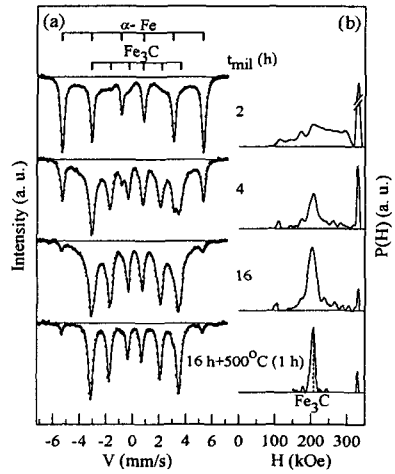

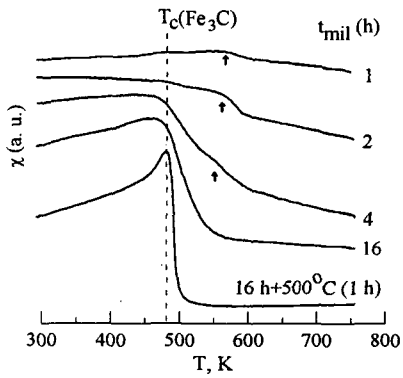

<u>The 1st stage</u>

Broadening bcc peaks of the α-Fe and formation of the amorphous (Am) Fe-C phase with the C concentration of 25at.%

<u>The 2nd stage</u>

Formation of the distorted $(Fe_3C)_D$ carbide.

α-Fe + C → Am (Fe-C) → $(Fe_3C)_D$

Quantitative analysis of the MA process in the Fe(75)C(25) mixture

t_{mil}, h	a(α-Fe), nm	$<L>_{\alpha\text{-Fe}}$, nm	f_{Am}, at.%	f_{if}, %
1	0.2867_3	7.5_5	20_3	35
2	0.2868_3	3.5_5	40_3	60

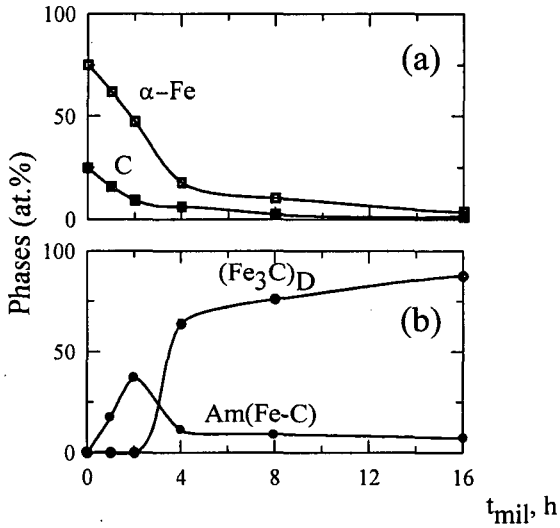

1. All solid state reactions take place on α-Fe reaching a nanocrystalline state.
2. C atoms penetrate along the grain boundaries and form in the interfaces (boundaries and close-to-boundary distorted zones) amorphous phase. According to (Horita et al. Mater. Charact. 37 (1996) 285; Yelsukov et al. Nanostruct. Mater. 12 (1999) 483; Phys. Met. Metallogr. 91 (2001) 46) the width of the interface can be estimated to be d≅1nm.
3. On reaching the fraction of interfaces the maximum value (~60%) and the C concentration in them of 25 at.%

the transition Am (Fe-C) → $(Fe_3C)_D$

takes place though amount of the reacted carbon is only 40% out of the total C amount in the initial mixture.

Mechanical alloying Fe(100-x)C(x); x=5-25 at.%
Final products (t_{mil}=16 hours)

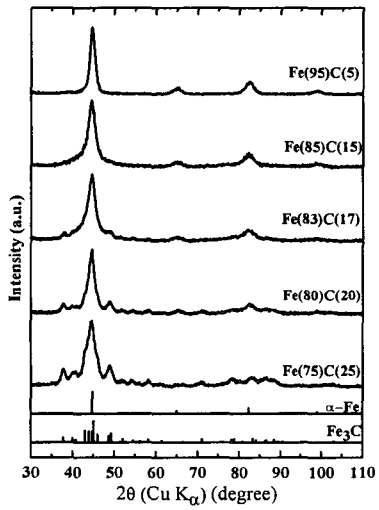

X-ray patterns

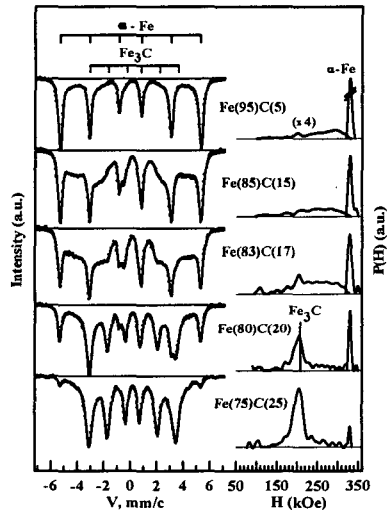

Mössbauer spectra and P(H) functions

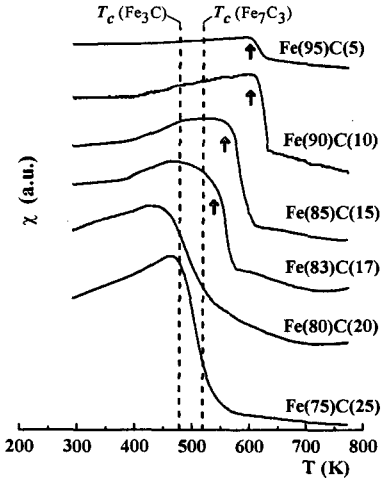

A.c. magnetic susceptibility

Phases

α-Fe+Am(Fe-C),	x≤15
α-Fe+Am(Fe-C)+$(Fe_3C)_D$,	=17
α-Fe+$(Fe_3C)_D$,	17<x<25
$(Fe_3C)_D$,	x=25

Quantitative analysis of the MA final products in the Fe(100-x)C(x) mixtures

A bcc lattice parameter (a) and grain size (<L>) of α-Fe, Curie temperature (T_C^{Am}), Fe atomic fraction (f_{Am}^{Fe}) and average HFMF (H_{Am}) of amorphous Fe-C phase

x, at.%	a, nm	<L>, nm	T_C^{Am}, K	f_{Am}^{Fe}	H_{Am}, kOe
5	0.2867_3	4.5_5	605_{10}	0.25_5	260_5
10	0.2871_3	3.5_5	615_{10}	0.40_5	250_5
15	0.2867_3	3.0_5	570_{10}	0.60_5	240_5
17	0.2871_3	2.5_5	550_{10}	0.70_5	235_5
20	–	–	–	0.28_5	–
25	–	–	–	0.10_5	–

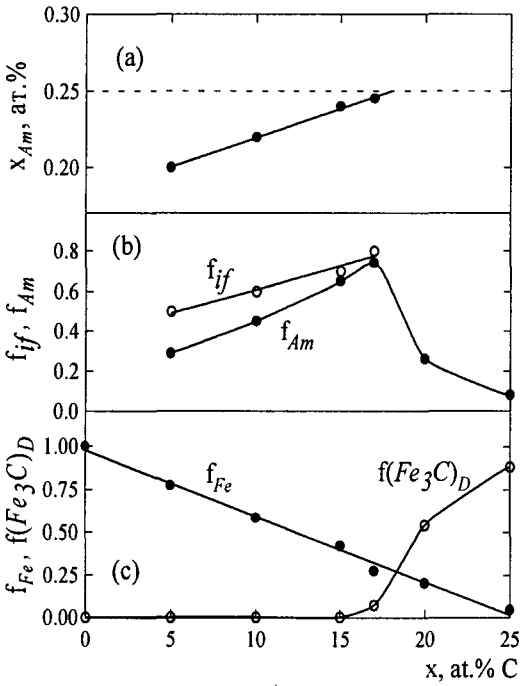

x_{Am} – C concentration in Am (Fe-C) phase (according to Bauer-Grosse and Le Caër Phil.Mag. B56 (1987) 485);

f_{Am} – atomic fraction of Am (Fe-C) phase;

f_{if} – volume fraction of interfaces from <L> and d_{if}=1 nm;

f_{Fe} – atomic fraction of nonreacted α-Fe;

$f(Fe_3C)_D$ – atomic fraction of the distorted Fe_3C carbide.

Mechanical alloying Fe-B system

1. H.Okumura et al, J. Mater. Sci., 27 (1993) 153.
2. A.Calka et al, Mater. Sci. Engen., A133 (1991) 555.
3. J.Jing et al, J.Phys.: Condens. Matter, 3 (1991) 7413.
4. V.A.Barinov et al, Phys. Met. Metallogr., 74(4) (1992) 412.
5. J.Balogh et al, J.Appl. Phys., 77(10) (1995) 4997.
6. E.C.Passamani et al, J.Phys.: Condens. Matter, 14 (2002) 1975.

The main results

1. $x \approx 20$ at.% B. One-stage process of MA

$$Fe + B \rightarrow Am(Fe\text{-}B) + Fe$$

2. $x \geq 30$ at.% B. Two-stage process of MA

$$Fe\text{-}B \rightarrow Fe + Am(Fe\text{-}B) \rightarrow Fe + Borides\ (Fe_2B \text{ and } FeB)$$

Mechanical alloying Fe(85)B(15)

X-ray patterns

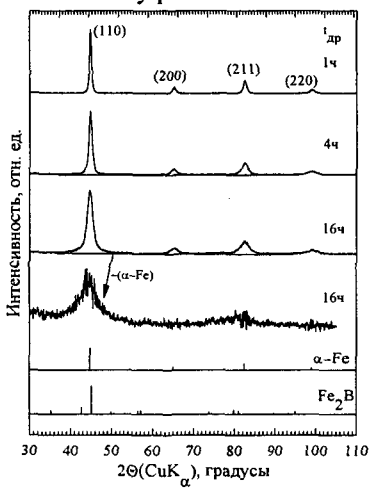

Mössbauer spectroscopy

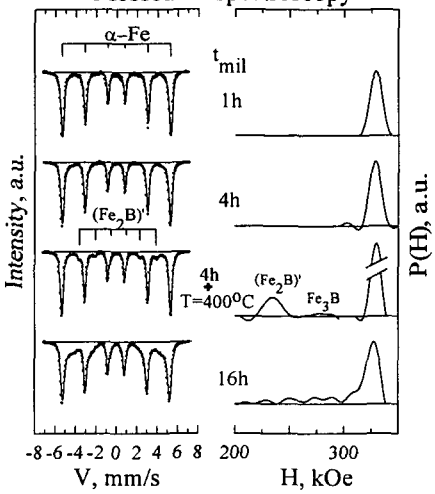

A.c. magnetic susceptibility temperature dependence of the sample after MA(16h) and followed by annealing at 400°C(1h)

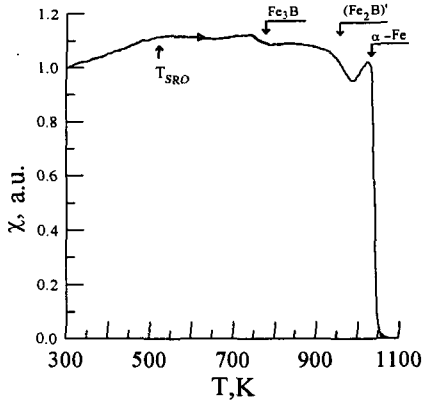

MA

Fe+B

↓

amorphous Fe-B phase + Fe

B concentration in amorphous phase is equal to about 20 at.%

MA + 400°C(1h)

α-Fe + $(Fe_2B)'$ + Fe_3B

Mechanical alloying Fe(85)B(15)

Quantitative analysis

Comparison with MA Fe(85)C(15)

Individual properties of B and C (graphite)

sp-element	Density, g/sm^3	Lattice type	Covalent radius, nm	Melting temperature, K	Enthalpy of vaporization, kJ/mole
B	2.34	tetragonal	0.88	2573	539
C	2.36	hexagonal	0.77	>4000	711

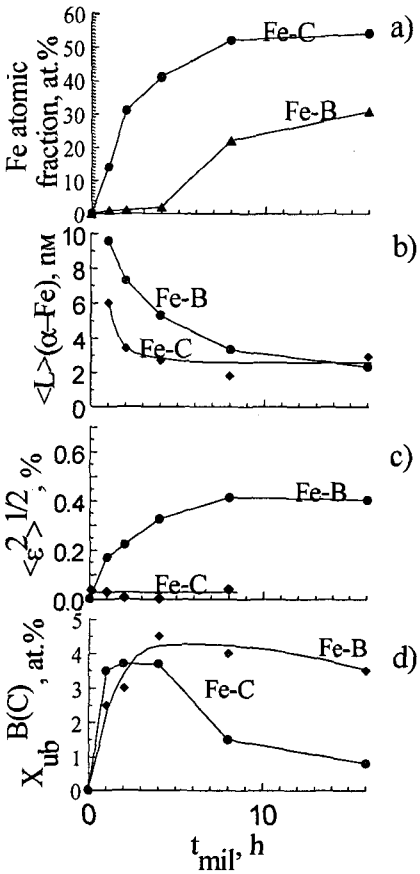

X^{B}_{Am} - B amount in the amorphous phase after MA;

X^{B}_{400} - B amount in the $(Fe_2B)'$ and Fe_3B borides after MA and followed by annealing at $T_{ann} = 400°C$ (1h)

t_{mil}, h	X^{B}_{Am}, at.%	X^{B}_{400}, at.%
0	0	0
1	0	2.5
2	0	3.0
4	0.5	5.0
8	5	9.0
16	7.5	11.0

$X^{B}_{ub} = X^{B}_{400} - X^{B}_{Am}$ - amount of B unbound in the α-Fe particles after MA

Comparative analysis of MA in Fe-Si, Fe-Ge and Fe-Sn systems

1. E.P.Yelsukov et al, Mater. Sci. Forum, 269-272 (1998) 151.
2. G.A.Dorofeev et al, in Mössbauer Spectroscopy in Materials Science, Edited by M.Miglierini and D.Petridis, Kluwer, the Netherlands, 1999, p.151.
3. G.A.Dorofeev et al, Mater. Sci. Forum, 343-346 (2000) 585.
4. G.A.Dorofeev et al, Phys. Met. Metallogr., 91(1) (2001) 47.
5. E.P.Elsukov et al, Phys. Met. Metallogr., 93(3) (2002) 93.
6. E.P.Elsukov et al, Phys. Met. Metallogr., 95(2) (2003) 60.
7. E.P.Elsukov et al, Phys. Met. Metallogr., 95(5) (2003) 486.
8. C.Bansal et al, J.Appl. Phys., 76 (1994) 5961.
9. E.Gaffet et al, J.Alloys. Compd., 194 (1993) 339.
10. M.Abdellaoui et al, J.Alloys. Compd., 198 (1993) 155.
11. M.Abdellaoui et al, Mater. Sci. Fofum, 179-181 (1995) 109.
12. N.Ševulova et al, J.Magn. Magn. Mater., 203 (1999) 190.
13. A.F.Cabrera et al, Mater. Sci. Forum, 312-314 (1999) 85.
14. S.Sarkar et al, Phys. Rev. B, 62 (2000) 3218.
15. A.F.Cabrera and F.H.Sanchez, Phys. Rev. B, 65 (2002) 094202-1.
16. S.Nasu et al, Hyperfine Interact., 55 (1990) 1043.
17. S.Nasu et al, Mater. Sci. Forum, 88-90 (1992) 569.
18. G.Le Caër et al, Mater. Sci. Forum, 179-181 (1995) 469.
19. M.O.Kientz et al, NanoStruct. Mater., 6 (1995) 617.

The main results

1. At the first stage an intermetallic compound in the amorphous or nanocrystalline modifications is formed.
2. At the second stage – SSS of the Si (Ge, Sn) concentration in the initial mixtures does not exceed 32 at.%.
3. Sharply decreasing intensity of Si, Ge and Sn reflections without changing their positions in X-ray patterns.

Mechanical alloying Fe(68)Si(32)

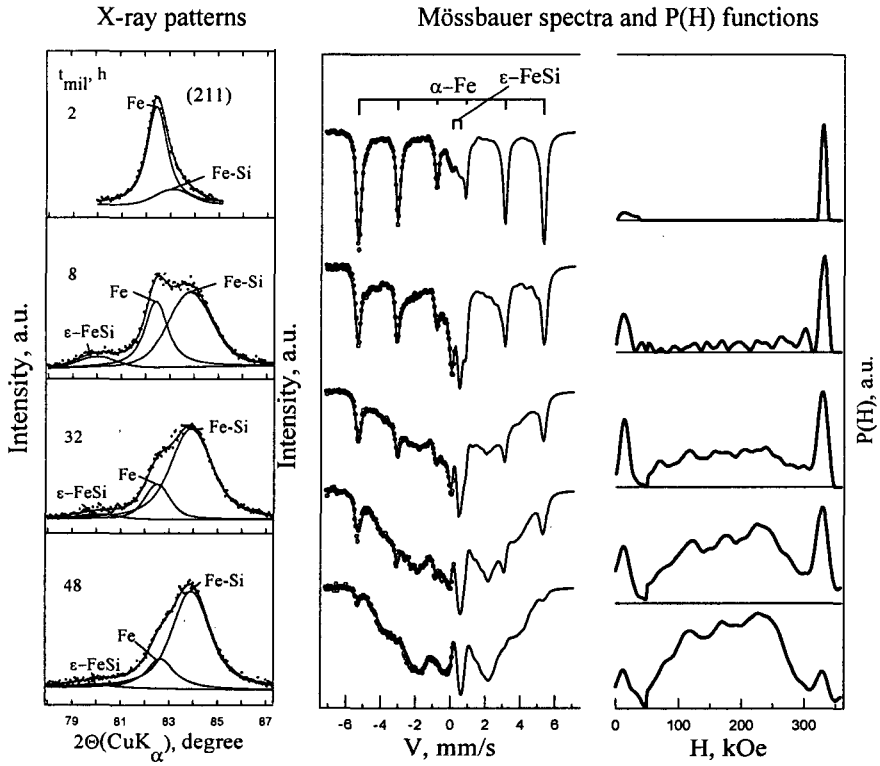

The 1st stage

Broadening bcc peaks of the α-Fe and the formation of the ε-FeSi intermetallic compound

The 2nd stage

The formation of the α-Fe(Si) supersaturated solid solution

Mechanical alloying Fe(68)Ge(32)

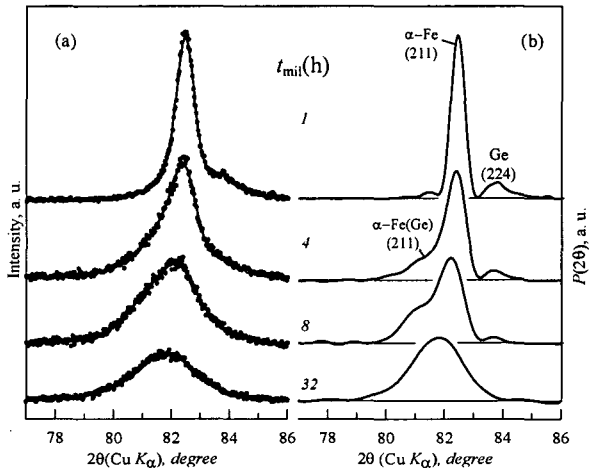

X-ray patterns

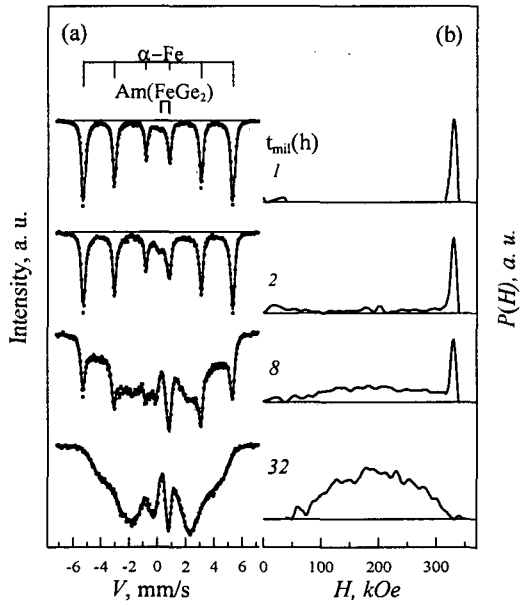

Mössbauer spectra and P(H) functions

Mechanical alloying Fe(68)Sn(32)

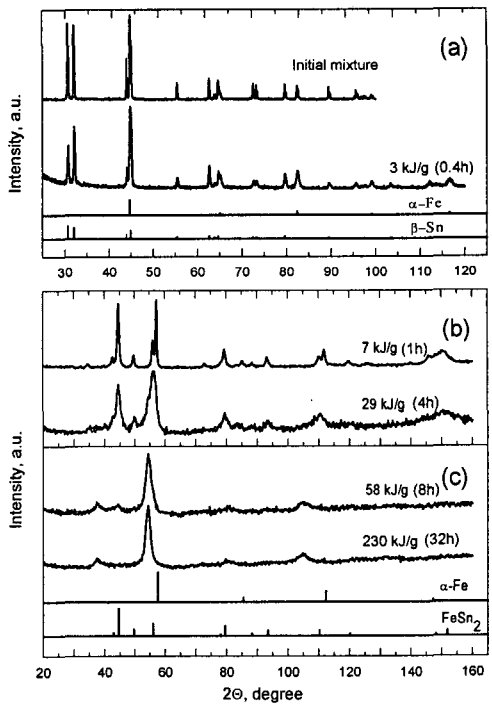

X-ray diffraction patterns as a function of dose. At the bottom the dash patterns of some phases are shown.

(a) - (0 - 4 kJ/g); Cu K_α radiation. The initial stage of mechanical alloying without new phases formation.

(b) - (4 - 30 kJ/g); Fe K_α radiation. The stage of $FeSn_2$ intermetallic compound formation.

(c) - (30 - 230 kJ/g). Fe K_α radiation. The final stage of the mixture transformation into the only phase of the bcc supersaturated solid solution based on α-Fe.

Mechanical alloying Fe(68)Sn(32)

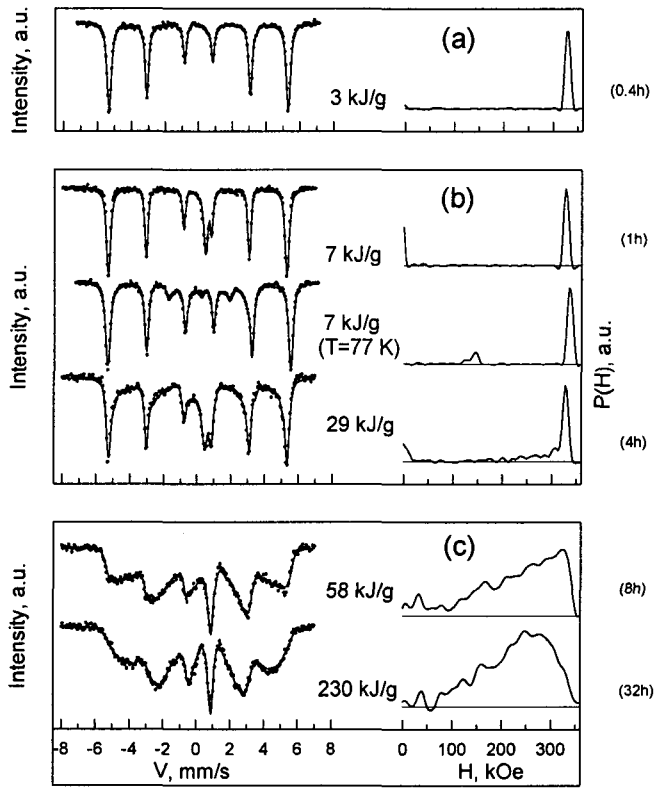

^{57}Fe Mössbauer spectra with the corresponding hyperfine field distributions P(H) as a function of dose. The isomer shifts relatively α-Fe at room temperature.

(a) - (0 - 4 kJ/g). The initial stage of mechanical alloying without new phases formation.

(b) - (4 - 30 kJ/g). The stage of $FeSn_2$ intermetallic compound formation.

(c) - (30 - 230 kJ/g).. The final stage of the mixture transformation into the only phase of the bcc supersaturated solid solution based on α-Fe.

Mechanical alloying Fe(68)Sn(32)

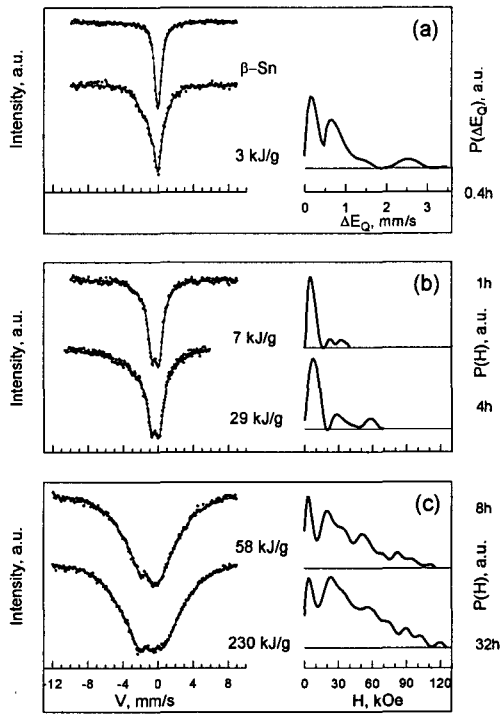

^{119}Sn Mössbauer spectra with the corresponding hyperfine parameter distributions as a function of dose. The isomer shifts relatively β-Sn at room temperature.

(a) - (0 - 4 kJ/g). The initial stage of mechanical alloying without new phases formation.

(b) - (4 - 30 kJ/g). The stage of $FeSn_2$ intermetallic compound formation.

(c) - (30 - 230 kJ/g).. The final stage of the mixture transformation into the only phase of the bcc supersaturated solid solution based on α-Fe.

The milling time dependences of the phases amount - (a) and (b), grain size of the α-Fe - (c), Si(Ge, Sn) concentration in supersaturated solid solution - (d)

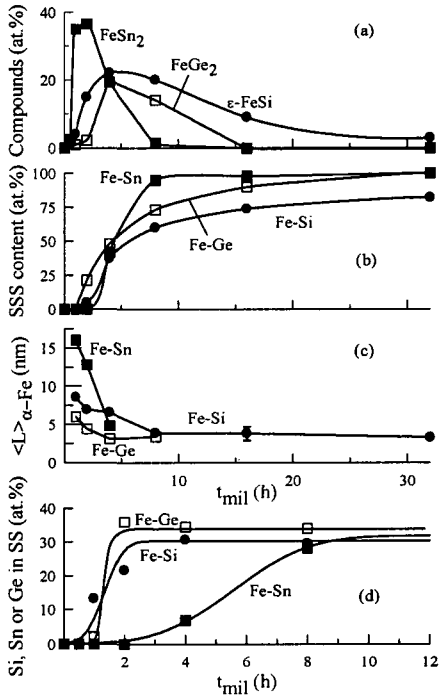

1. All solid state reactions take place on α-Fe reaching a nanocrystalline state.
2. The sp-element type influences the kinetics:

- intermetallic compound and α-Fe(Sn) solution are formed faster than those in Fe-Si and Fe-Ge systems;
- a different situation takes place in the saturation of solid solution. In the Fe-Ge and Fe-Si systems the maximum Ge (Si) concentration sets in simultaneously with the formation of the solid solution. In the Fe-Sn system the solid solution is saturated with Sn gradually.

Comparative analysis of MA in Fe-Al and Fe-Si systems Mechanical alloying in Fe-Al system

1. C.Bansal et al, J.Appl. Phys., 76 (1994) 5961.
2. P.H.Shingu et al, in New Materials by Mechanical Alloying Techniques, Edited by E.Artz and L.Schultz (DGM Informationgeselschaft, Oberursel, 1989) p.319.
3. W.H.Wang et al, J.Non-Cryst. Sol., 124 (1990) 82.
4. G.M.Wang et al, J.Magn. Magn. Mater., 97 (1991) 73.
5. Y.D.Dong et al, Mater. Sci. Eng., A134 (1991) 867.
6. W.Guo et al, Mater. Sci. Forum, 89-90 (1992) 139.
7. E.Bonetti et al, J.Appl. Phys., 74(3) (1993) 2058.
8. V.F.Fadeeva et al, Mater. Sci. Forum, 179-181 (1995) 397.
9. E.Bonetti et al, J. Appl. Phys., 79(10) (1996) 7537.
10. S.Enzo et al, Acta Mater., 43 (1996) 3105.
11. S.Enzo et al, Mater. Sci. Forum, 269-272 (1998) 385.
12. S.Enzo et al, Mater. Sci. Forum, 269-272 (1998) 391.
13. K.Wolski et al, Mater. Sci. Eng., A207 (1996) 97.
14. E.Jartych et al, Hyperfine Interact., 99 (1996) 389.
15. D.Oleszak et al, in Rapidly Quenched and Metastable Materials, Supplement, Edited by P.Duhaj, P.Mrafko and P.Svec, Elsevier, Notherlands, 1997, p.18.
16. D.Oleszak and P.H.Shingu, Mater. Sci. Forum, 235-238 (1997) 91.
17. D.Oleszak et al, Mater. Sci. Forum, 269-272 (1998) 643.
18. E.Jartych et al, J.Phys.: Condens. Matter, 10 (1998) 4929.
19. D.E.Eelman et al, J.Alloys Compd., 266 (1998) 234.
20. M.Hashii, Mater. Sci. Forum, 312-314 (1998) 139.
21. M.Hashii and K.Tokumitsu, Mater. Sci. Forum, 312-314 (1999) 399.
22. G.Gonzales et al, Mater. Sci. Forum, 360-362 (2001) 349.
23. E.P.Yelsukov et al., Acta Mater. 52(2004) 4251.

Mechanical alloying in Fe-Al system

The main results

1. MA is carried out under the condition of reaching a nanocrystalline state (<L> < 10nm).

2. At the first stage of MA the amorphous Am(Fe_2Al_5) phase is formed. In some papers this phase is supposed to be formed due to Fe dissolution into Al.

3. The formation of the α-Fe(Al) SSS takes place with x≤60 at.% Al.

4. The Al concentration in SSS from the very beginning of its formation is close to that in the initial mixture.

Mechanical alloying Fe(68)Al(32)

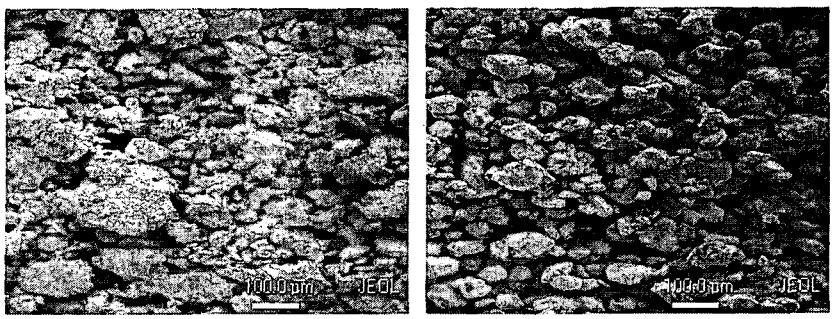

t_{mil}=1 h t_{mil}=16 h

Secondary electron microscopy mode image of particles

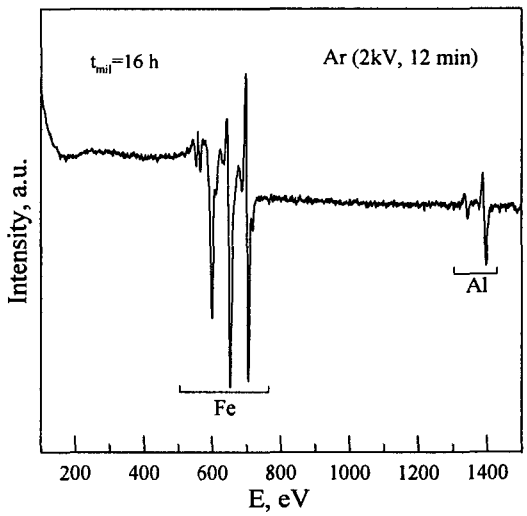

Auger-spectrum of the powder after etching the surface layer of 30 nm thick

Mechanical alloying Fe(68)Al(32)

Chemical composition of surface layers (SIMS) and bulk (CA) of particles.

t_{mil}, h	Concentration, at.%					Method of determination
	Fe	Al	Cr	C	O	
0.5	33±2	67±4	< 0.1	< 0.1	< 0.1	SIMS
0.5	68.8±2	31.1±1	< 0.01	-	-	CA
1	48±3	52±3	< 0.1	< 0.1	< 0.1	SIMS
1	68.5±2	31.5±1	< 0.01	-	-	CA
16	67±3	33±2	< 0.1	< 0.1	< 0.1	SIMS
16	68.7±2	31.3±1	< 0.01	-	-	CA

Mechanical alloying in Fe(68)Al(32) system

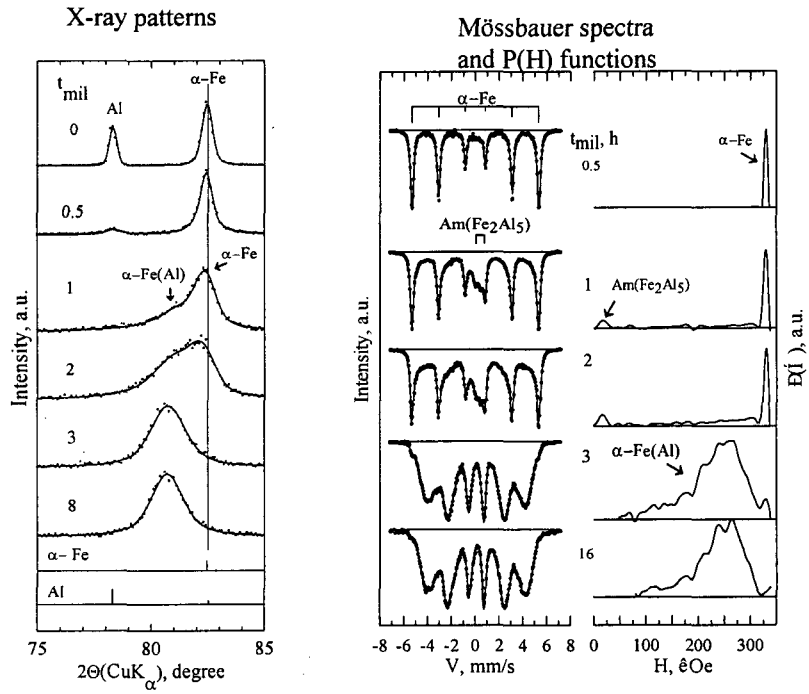

The 1st stage

Broadening reflections of α-Fe and sharp decreasing intensity of Al reflections without change their positions, formation of the $Am(Fe_2Al_5)$ intermetallic compound

The 2nd stage

The formation of the α-Fe(Al) supersaturated solid solution

Mechanical alloying Fe(68)Al(32)

attice parameter (a) and average hyperfine magnetic field ($\overline{H}$) of the α-Fe(Al) solid solution

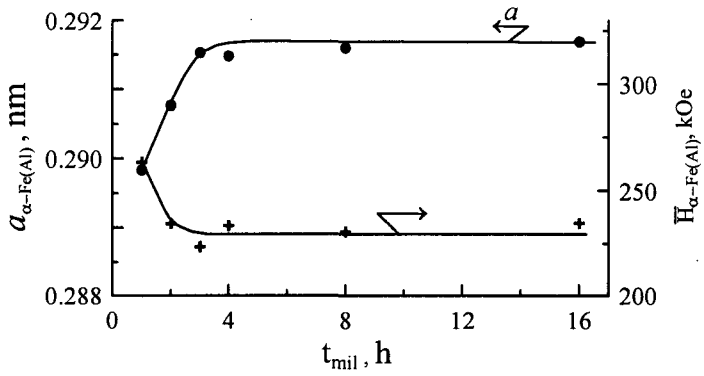

A.c. magnetic susceptibility (χ) of samples with t_{mil} = 4 and

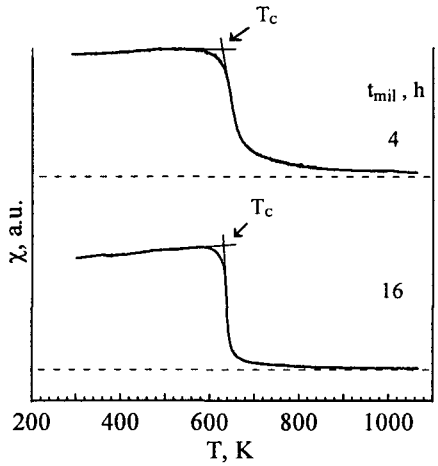

T_C=625 K corresponds to 31 at/% Al

Comparative analysis of the MA process in the Fe(68)Al(32) and Fe(68)Si(32) mixtures

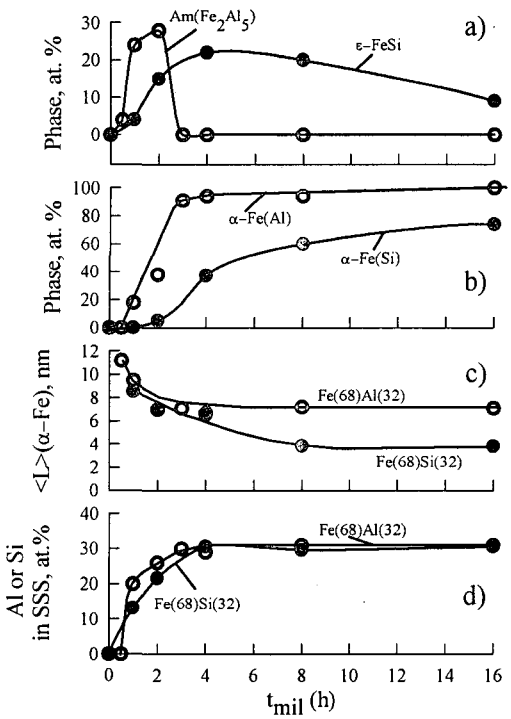

Intermetallic compound amount

α-Fe(Al) and α-Fe(Si) amount

Grain size of α-Fe

Al and Si concentration in supersaturated solid solution

1. All SSRs take place on α-Fe reaching a nanocrystalline state
2. Kinetics of SSRs in Fe-Al system is much faster than those in Fe-Si one
3. The maximum Al or Si concentration in SSS sets in simultaneously with its formation

Mechanical alloying Fe(68)M(32); M=Al, Si, Ge, Sn

Pure element content according to the X-ray data

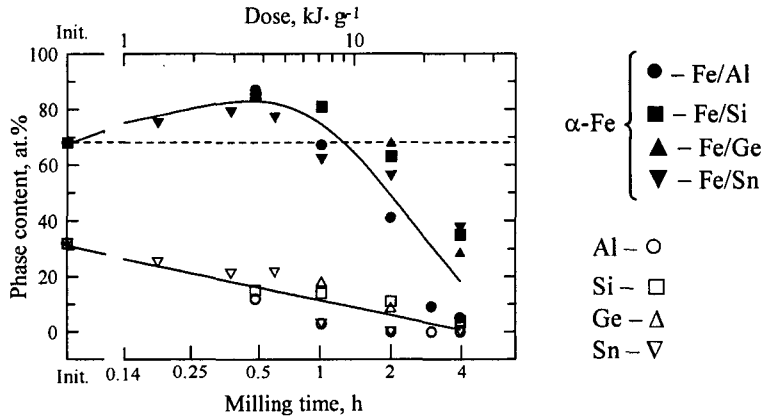

Increasing the α-Fe content and decreasing the sp-element content at a short milling time are an evidence of M atom penetration along the α-Fe grain boundaries.

Segregations of M atoms (x^M_{ub})

$$x^M_{ub}(t_{mil}) = x^M(0) - [x^M(t_{mil}) + x^M_{IC}(t_{mil}) + x_{SSS}(t_{mil})]$$

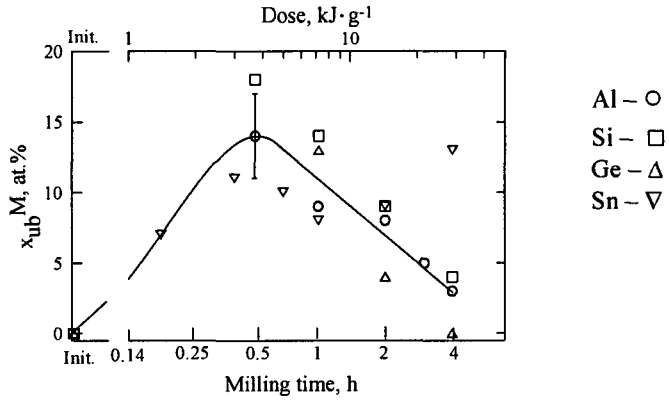

Mechanical alloying Fe(93)Mg(7)

1. A.Hightower et al., J. Alloys Compds. 252(1997) 238
2. G.A.Dorofeev et al., Inorganic Mater. (Russia) 7(2004)

The main results

1. Possibility of obtaining the α-Fe(Mg) supersaturated solid solution with Mg concentration of about 5-7 at.% has been shown.

2. There are no data on the atomic mixing kinetics for the mixture content with which complete solving takes place.

MECHANICAL ALLOYING Fe(93)Mg(7)

Secondary electron microscopy mode image of particles

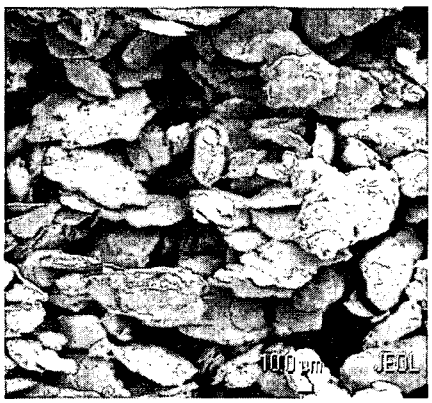

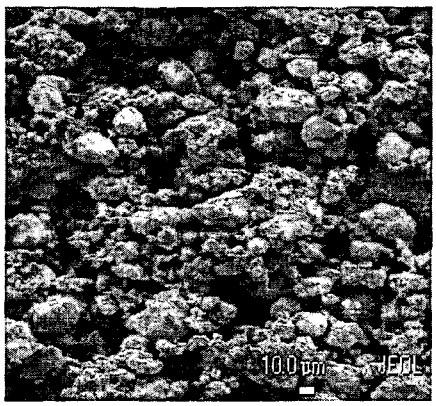

t_{mil} = 1h
Disc-like shape: D≈80 µm, h=1-5 µm

t_{mil}= 16h
Stone-like shape: D≈10-50 µm

Chemical composition of surface layer (SIMS) and bulk (CA) of particles

t_{mil}, h	Concentration, at.%		Method of determination
	Fe	Mg	
1	71±3	29±2	SIMS
	94±2	6.0±0.5	CA
16	93±3	7±1	SIMS
	94±2	6.0±0.5	CA

MECHANICAL ALLOYING Fe(93)Mg(7)

X-ray diffraction

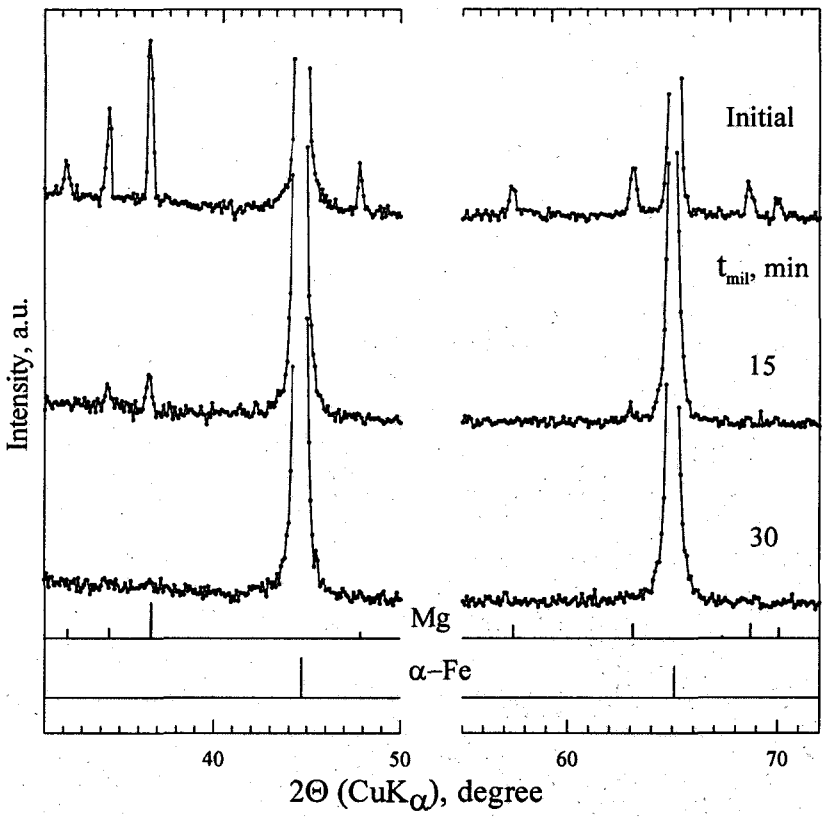

Drastic decreasing intensity of Mg reflections without changing their positions

MECHANICAL ALLOYING Fe(93)Mg(7)

X-ray diffraction

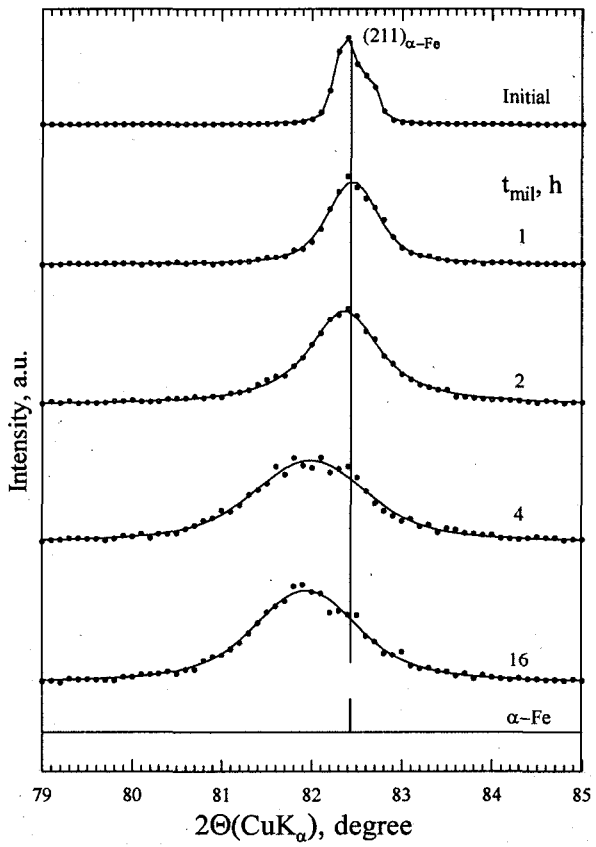

Broadening BCC reflections and their shift toward the smaller 2θ degrees

MECHANICAL ALLOYING Fe(93)Mg(7)

Mössbauer spectroscopy

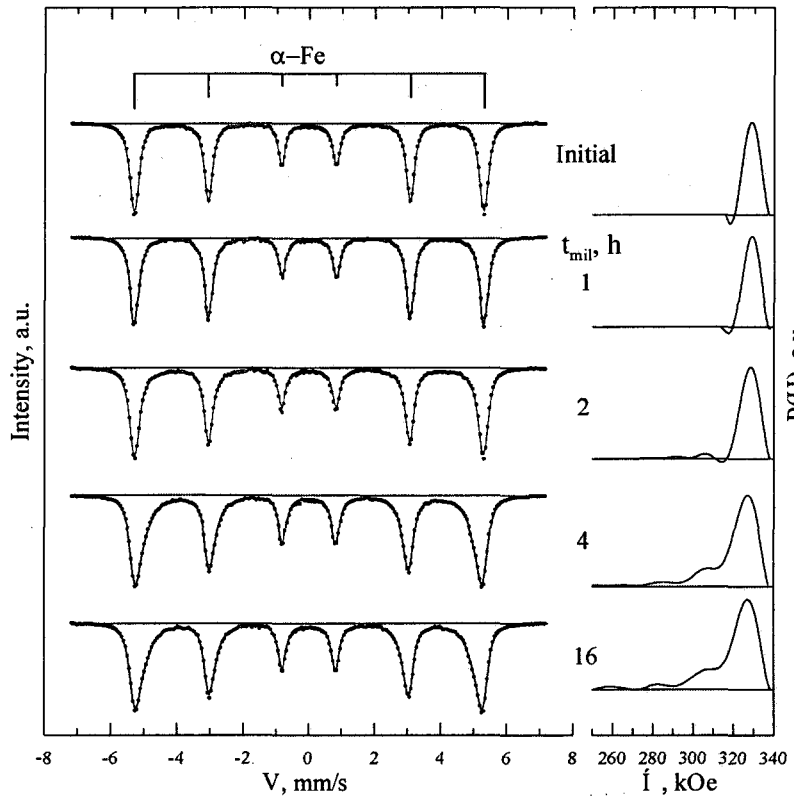

The new components appear
in the Mössbauer spectra and P(H) functions at $t_{mil} \geq 2h$.

The formation of the α-Fe(Mg) supersaturated solid solution.

The Mg concentration in SSS is estimated to be of 5-6 at.%
according to the Mössbauer data.

MECHANICAL ALLOYING Fe(93)Mg(7)

Quantitative analysis

Reduced amount of Mg

BCC lattice parameter

Grain size and microstrain of BCC phase

Average hyperfine magnetic field

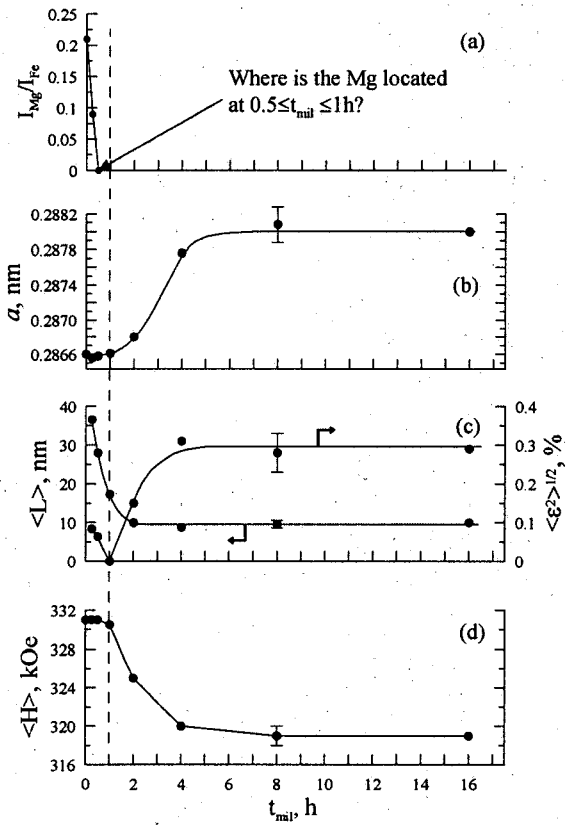

- The α-Fe(Mg) formation takes place on α-Fe reaching a nanocrystalline state (t_{mil}>1h).
- MA process is virtually completed by t_{mil}=4h.

MECHANICAL ALLOYING Fe(93)Mg(7)

X-ray diffraction (t_{mil}=1h)

On the supposition that all Mg is located on the α-Fe particles surface, thickness of the Mg layer have to be of 0.13 μm.

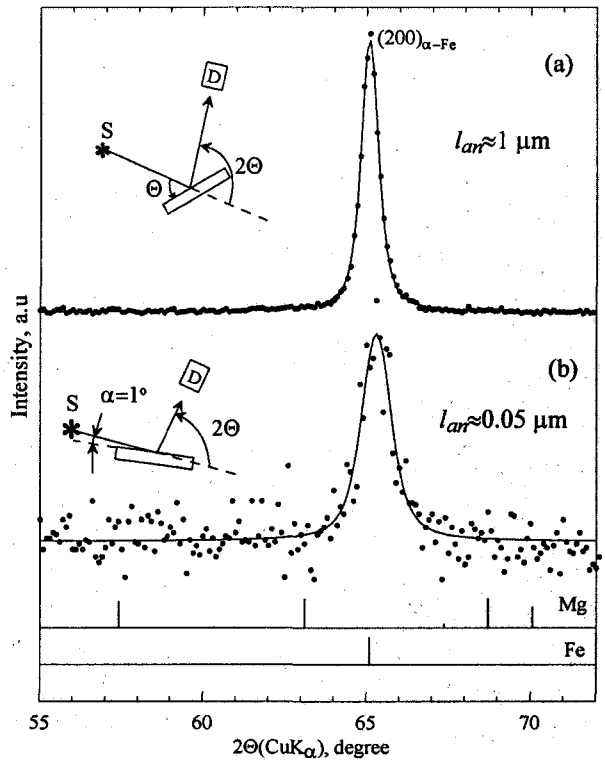

The Mg atoms are segregated at the α-Fe grain boundaries

Model of deformation atomic mixing Fe/M; M=B,C,Al,Si,Ge,Sn,Pb

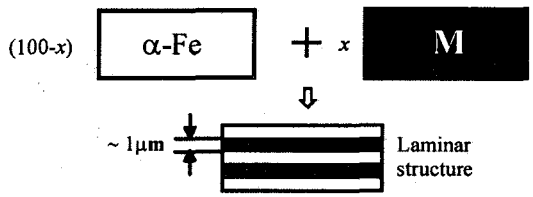

The 1st stage of MA

1. Formation in α–Fe of nanostructure (<L> < 10 nm) and interfaces containing boundary (——) and close-to-boundary distorted zone (▨)

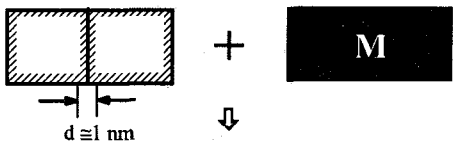

2. Penetration of M atoms along grain boundaries, their segregation (▬▬) and decreasing <L>

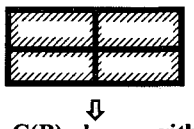

3. Formation of amorphous Fe-C(B) phases with 20-25 at.% C(B) and Am(Fe_2Al_5), ε– FeSi, Am($FeGe_2$), $FeSn_2$ intermetallic compounds with amorphous or nanocrystalline structures in interfaces (▩); formation of a-Fe (Mg, Pb) SSS if $x < 7$ at.%

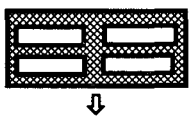

The 2nd stage

4. Formation of the Fe_3C and Fe_7C_3 carbides, Fe_2B boride if $15<x\leq32$ at.% C(B), α–Fe(M) SSS if $x\leq32$ at.% Si(Ge, Sn) and $x\leq60$ at.% Al.

[E.P. Yelsukov and G.A. Dorofeev, J. Mater. Sci. 39(2004)5071.]